Anal. Chem. **2010,** *82,* 5317–5322

Snapshot Voltammetry Using a Triangular Bipolar Microelectrode

Byoung-Yong Chang, François Mavré,† Kwok-Fan Chow, John A. Crooks, and Richard M. Crooks*

Department of Chemistry and Biochemistry, Center for Electrochemistry, and the Center for Nano- and Molecular Science and Technology, The University of Texas at Austin, 1 University Station, A5300, Austin, Texas 78712-0165

In this paper, we report a new electroanalytical technique we call snapshot voltammetry. This method combines the properties of bipolar electrodes with electrogenerated chemiluminescence (ECL) to provide a means for recording optical voltammograms in a single micrograph. In essence, the information in a snapshot voltammogram is contained in the spatial domain rather than in the time domain, which is the case for conventional voltammetry. The use of a triangle-shaped bipolar electrode stabilizes the interfacial potential difference along its length. Basic electrochemical parameters extracted from snapshot voltammograms are in good agreement with those obtained by conventional voltammetry. Although not explicitly demonstrated in this paper, this method offers the possibility of using arrays of bipolar electrodes to obtain numerous snapshot voltammograms simultaneously.

Here we report a new electroanalytical method, which we call snapshot voltammetry, that produces a complete voltammogram from a single optical image of the electrogenerated chemiluminescence (ECL) emitted from a triangular bipolar electrode (BPE).[1−6] BPEs are electronically conductive wires immersed in an ionically conductive phase. When a sufficiently high voltage is applied across the electrolyte solution in contact with the wire, electrochemical oxidation and reduction reactions occur at the two ends of the wire. Importantly, no direct electrical contact to the BPE is required to initiate these faradaic reactions. In the experiment discussed here, the ECL reaction occurs at the anodic end of the BPE and the faradaic reaction of interest occurs at the cathode.[1,4] Because the rates of the oxidation and reduction reactions are the same at the two ends of the BPE, there is a direct relationship between the rate of the cathode reaction and the intensity of the emitted ECL.[6]

A significant difference between BPEs and the more common working electrodes used in three-electrode cell configurations is that a range of interfacial potential differences exists across the surface of BPEs due to the potential gradient present within the contacting solution.[6,11,12] Therefore, the ECL intensity is a function of the axial location of the emission, and hence it is possible to correlate multiple interfacial potential differences to ECL emission intensity. The important advantage of snapshot voltammetry is that all of the electrochemical data are contained in a single luminescence image of the BPE, and therefore a voltammogram can be obtained in a matter of seconds. Additionally, extension of this methodology to an array format, involving hundreds or thousands of electrodes, is quite easy to envision,[5] and therefore, it might be possible to use this approach for high-throughput electrochemical analyses.

A significant theme in our recent reports relating to BPEs is that ECL emission can be coupled to an electrochemical reaction of interest, and that the emission intensity is a reliable reporter of the rate of the coupled reaction.[1,4] For example, we demonstrated that a single pair of driving electrodes and a single simple power supply could be used to simultaneously control electrochemical reactions at up to 1000 BPEs.[5] We have also presented a theoretical study correlating the current profile and ECL emission at a BPE to the applied potential.[6] These experiments have shown that the deformation of the electric field by faradaic reactions on the BPE will be negligible if the conductivity of the electrolyte solution is high (as is the case in the present study). Finally, we have also shown that BPEs can be used to control the local electric field within microchannels filled with an electrolyte of low conductivity,[7] and these findings have led to a new means for concentrating analytes via a process we call bipolar electrode focusing.[8−10]

In addition to our studies, there are several other contemporary reports of electroanalytical aspects of BPEs. For example, Duval and co-workers have presented a rigorous mathematical analysis of the potential profile at the interface of a BPE within the context of the Butler−Volmer kinetic formalism.[2] In an experiment more closely related to our work, Björefors and co-workers measured the potential gradient of the solution above a BPE using imaging

* To whom correspondence should be addressed. E-mail: crooks@cm.utexas.edu. Phone: 512-475-8674. Fax: 512-475-8651.

† Present address: Bâtiment Lavoisier bureau 719, Laboratoire d'Electrochimie Moléculaire, Université Paris Denis Diderot, 15 rue Jean de Baïf 75205 Paris Cedex 13, France.

(1) Zhan, W.; Alvarez, J.; Crooks, R. M. *J. Am. Chem. Soc.* **2002**, *124*, 13265–13270.

(2) Duval, J.; Kleijn, J. M.; van Leeuwen, H. P. *J. Electroanal. Chem.* **2001**, *505*, 1–11.

(3) Arora, A.; Eijkel, J. C. T.; Morf, W. E.; Manz, A. *Anal. Chem.* **2001**, *73*, 3282–3288.

(4) Chow, K.-F.; Mavré, F.; Crooks, R. M. *J. Am. Chem. Soc.* **2008**, *130*, 7544–7545.

(5) Chow, K.-F.; Mavré, F.; Crooks, J. A.; Chang, B.-Y.; Crooks, R. M. *J. Am. Chem. Soc.* **2009**, *131*, 8364–8365.

(6) Mavré, F.; Chow, K.-F.; Sheridan, E.; Chang, B.-Y.; Crooks, J. A.; Crooks, R. M. *Anal. Chem.* **2009**, *81*, 6218–6225.

(7) Perdue, R. K.; Laws, D. R.; Hlushkou, D.; Tallarek, U.; Crooks, R. M. *Anal. Chem.* **2009**, *81*, 10149–10155.

(8) Dhopeshwarkar, R.; Hlushkou, D.; Nguyen, M.; Tallarek, U.; Crooks, R. M. *J. Am. Chem. Soc.* **2008**, *130*, 10480–10481.

(9) Hlushkou, D.; Perdue, R. K.; Dhopeshwarkar, R.; Crooks, R. M.; Tallarek, U. *Lab Chip* **2009**, *9*, 1903–1913.

(10) Laws, D. R.; Hlushkou, D.; Perdue, R. K.; Tallarek, U.; Crooks, R. M. *Anal. Chem.* **2009**, *81*, 8923–8929.

10.1021/ac100846v
Published on Web 05/27/2010

surface plasmon resonance spectroscopy and electrochemical methods.[11,12] Specifically, they took advantage of this potential gradient to partially desorb a thiolated self-assembled monolayer (SAM) previously deposited on the BPE. The resulting SAM exhibited a density gradient along the BPE surface that tracked the strength of the local electric field. By applying different electric fields, different density patterns of molecules were formed on the BPE surface.[11,12] Finally, Manz and co-workers used a U-shaped BPE in a flow system to construct a wireless ECL device for detecting amino acids.[3]

In the present article, we describe how two key attributes of BPEs can be combined to create a snapshot voltammogram. First, the potential gradient across the BPE drives faradaic electrochemical reactions. Second, ECL reporting provides a means for visualizing the reaction rate as a function of axial position along the electrode. To demonstrate the principles of snapshot voltammetry, we examined the ECL intensity profile as a function of the axial location in a single ECL micrograph. Previously reported results make it possible to determine the interfacial potential as a function of location at the interface,[2,6] and with this information, the ECL intensity can be directly correlated to potential.[13,14] This is sufficient information to construct conventional voltammograms from the snapshot. To support this claim, we demonstrate that key voltammetric parameters, including the half-wave potential ($E_{1/2}$) and the number of electrons transferred (n), can be extracted from snapshot voltammograms for oxidation of $Ru(bpy)_3^{2+}$ (bpy = 2,2′-bipyridine) in the presence of different co-reactants.

EXPERIMENTAL SECTION

Chemicals. The following chemicals were purchased and used as received unless otherwise noted in the text: $Ru(bpy)_3Cl_2 \cdot 6H_2O$ and tri-*n*-propylamine (TPrA) from Sigma-Aldrich (Milwaukee, WI) and oxalic acid from J.T. Baker (Phillipsburg, NJ). All solutions contained 5.0 mM $Ru(bpy)_3^{2+}$, 25.0 mM TPrA or 6.6 mM oxalic acid, and 0.10 M phosphate buffer (pH = 6.9). Milli-Q water (Milli-Q reagent water system, Millipore, Bedford, MA) was used to prepare all aqueous solutions.

Device Fabrication. Au electrodes on glass slides were prepared using standard photolithographic methods described in our previous reports.[1,4] Briefly, a positive photoresist layer (~10 μm thick, AZ P4620, AZ Electronic Materials, Somerville, NJ) was spin-coated onto Au-coated glass (5 nm Cr adhesion layer and 100 nm Au top layer, EMF Corp., Ithaca, NY) and exposed to UV light through a positive photomask containing the electrode design. After it was developed (AZ 421 K, AZ Electronic Materials) for 2 min to remove the exposed photoresist layer, the Au layer was removed by immersion into an aqueous solution containing 5% I_2 and 10% KI (w/v) for 2 min, and the Cr adhesion layer was subsequently etched for 30 s using an aqueous solution containing 9% $(NH_4)_2Ce(NO_3)_6$ (w/v) and 6% $HClO_4$ (v/v).[15] Finally, the remaining photoresist was removed with acetone.

Scheme 1

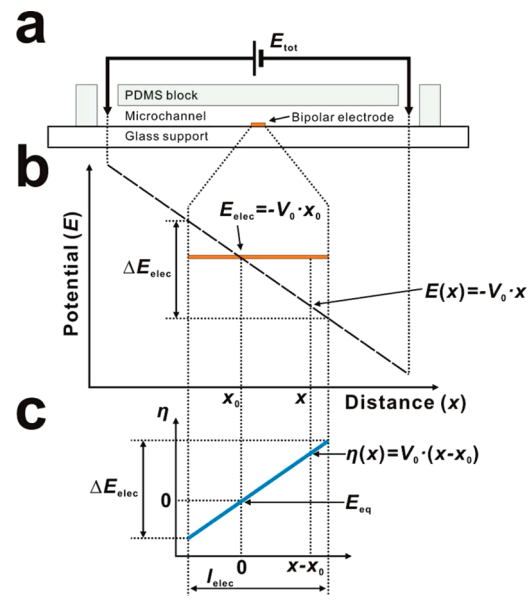

The poly(dimethylsiloxane) (PDMS) microfluidic channel was prepared from Sylgard 184 (Dow Corning, Midland, MI) by soft lithography.[16] The dimensions of the channel were 1.2 cm long, 1.75 mm wide, and 28 μm high. Two reservoirs, having diameters of 1.0 mm, were punched at the ends of the channel to accommodate introduction of solutions and the driving electrodes. The glass substrate and the PDMS microchannel were treated with an air plasma for 15 s (PDC-32G, Harrick Plasma, Ithaca, NY), pressed together, and then heated at 70 °C for 2 min to irreversibly bind them together.

Optical and Fluorescence Imaging. A microscope (Nikon AZ100, Nikon Co., Tokyo, Japan) equipped with a mercury lamp (Nikon) and a CCD camera (Cascade, Photometrics Ltd., Tucson, AZ) were used to obtain the optical and snapshot ECL micrographs. The latter were taken with an exposure time of 1.500 s. The ECL intensity profiles were obtained using V++ Precision Digital Imaging software (Digital Optics, Auckland, New Zealand). Three-dimensional (3D) image rendering was carried out using Matlab (The Mathworks, Natick, MA).

RESULTS AND DISCUSSION

Basic Principles. When a potential (E_{tot}) is applied between the two ends of a microchannel filled with an electrolyte solution, as depicted in part a of Scheme 1, the electric field (V_0) and the potential at a position (x,y) inside the channel are given by eqs 1 and 2.

$$V_0 = E_{tot}/l_{channel} \quad (1)$$

$$E(x,y) = E(x) = -V_0 x \quad (2)$$

Here, $l_{channel}$ is the length of the channel and $E(x,y)$ is a function only of x (the coordinate parallel to the channel length) because the y axis is perpendicular to the electric field.[17] Additional information relevant to this point is provided in the Supporting

(11) Ulrich, C.; Andersson, O.; Nyholm, L.; Björefors, F. *Angew. Chem., Int. Ed.* **2008**, *47*, 3034–3036.
(12) Ulrich, C.; Andersson, O.; Nyholm, L.; Björefors, F. *Anal. Chem.* **2009**, *81*, 453–459.
(13) Kanoufi, F.; Bard, A. J. *J. Phys. Chem. B* **1999**, *103*, 10469–10480.
(14) Kanoufi, F.; Zu, Y.; Bard, A. J. *J. Phys. Chem. B* **2001**, *105*, 210–216.
(15) Williams, K. R.; Gupta, K.; Wasilik, M. *J. Microelectromech. Syst.* **2003**, *12*, 761–778.
(16) Xia, Y.; Whitesides, G. M. *Angew. Chem., Int. Ed.* **1998**, *37*, 550–575.
(17) Fleischmann, M.; Ghoroghchian, J.; Rolison, D.; Pons, S. *J. Phys. Chem.* **1986**, *90*, 6392–6400.

Information. Part b of Scheme 1 is an idealized plot of potential (E) versus distance (x) in the channel, but it should be kept in mind that in reality a small percentage of E_{tot} is dropped at the driving electrodes.[6] Once an equilibrium potential between the BPE and the solution is established at x_0, which is the point where the potentials of the BPE (E_{elec}) and the solution ($E(x_0)$) are the same, the overpotential experienced by redox molecules in solution at position x is $\eta(x)$. The value of $\eta(x)$ is derived from the interfacial potential difference between the BPE and the solution (eqs 2−4).[18]

$$E(x_0) = -V_0 x_0 = E_{elec} \quad (3)$$

$$\eta(x) = E_{elec} - E(x) = E(x_0) - E(x) = V_0(x - x_0) \quad (4)$$

For x larger than x_0, $\eta(x)$ has a positive polarity leading to oxidizing potentials, and for x less than x_0, $\eta(x)$ has a negative polarity leading to reducing potentials. The value of $\eta(x)$ increases linearly along the x axis (part c of Scheme 1), while the solution potential, $E(x)$, decreases with x (part b of Scheme 1).

One final point: because snapshot voltammograms are derived from an optical response, they do not contain a non-faradaic, capacitive component. The situation is analogous to other types of spectroelectrochemical measurements in which an optical response is plotted as a function of electrode potential.

Experimental Configuration. It has previously been shown that the faradaic current through a BPE can be measured.[6,7,12] However, it has not been possible to directly determine the local current flowing between the electrode and solution at a specific location ($i(x)$) on the BPE. However, as we show here, ECL provides a convenient means to indirectly determine $i(x)$.[13,14,19]

For sensing purposes, ECL reporting is controlled by the rate of reduction at the cathode end of the BPE, which is directly dependent on the concentration of the oxidized species in solution.[1] However, in the present study, we focus specifically on characterizing the ECL reactions that occur at the anode of the BPE. Therefore, a triangular BPE was fabricated to optimize conditions for ECL reporting (Figure 1a). This triangular configuration is equivalent to using a counter electrode having a larger surface area than the working electrode in a conventional electrochemical cell.[18] Here, the wider side of the triangle was used as the counter electrode for reductions, and the tip of the triangle was used as the working electrode for the ECL reaction. Because the cathodic pole has a much larger surface area than the anodic pole, this configuration ensures that the rate of the ECL reaction is not limited by the corresponding reduction. We have previously shown that position x_0 will adjust itself to a new E_{elec} to maintain the balance between the total anodic and cathodic currents.[6] On a rectangular BPE, x_0 was observed to move toward the cathodic pole as the rate of the ECL reaction was increased by increasing the electric field. However, the larger cathode area of the triangular BPE compensates for this effect, and this ensures that x_0 remains constant over a broad range of values of E_{tot}. This is important because the x_0 value can be obtained directly from the data acquired under different electric field strengths, and it will be used as a reference point for defining the overpotential gradient on the BPE whose potential is floating.

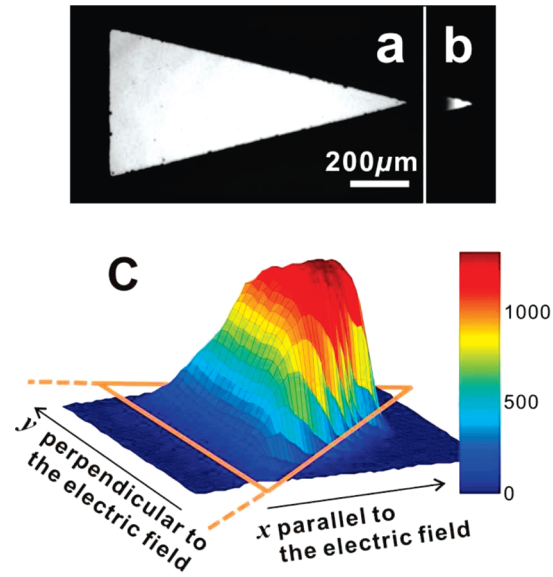

Figure 1. (a) Optical micrograph of the triangular BPE. (b) Two-dimensional luminescence micrograph. (c) Expanded three-dimensional rendering of the micrograph in (b). In (c), the luminescence intensity is displayed along the vertical axis, and the orange lines (not to scale) serve only to indicate that the image is a rendering of part of the triangular BPE tip. The scale bar in (a) also applies to (b). In (c), the vertical axis is given in counts per pixel (see Figure 3b). The region of the electrode represented in (c) is the same as that shown in (b). Conditions: E_{tot} = 25.0 V, and V_0 = 2.08 V/mm. The solution contained 5.0 mM $Ru(bpy)_3^{2+}$, 25.0 mM TPrA, and 0.10 M phosphate buffer (pH = 6.9).

ECL Intensity Profile upon Application of an Electric Field. Figure 1b is a two-dimensional (2D) luminescence micrograph obtained from the BPE shown in part a when E_{tot} = 25.0 V (V_0 = 2.08 V/mm) is applied across the channel. Note that the calculated value of V_0 (eq 1) is based on the assumption that the potential drop at the driving electrodes is negligible.[4] Figure 1c is an expanded, 3D rendering of part b. As discussed previously, the ECL intensity is only dependent on the axis parallel to the electric field (x axis). The intensity along the y axis, which is perpendicular to the electric field, is constant. Accordingly, the BPE can be regarded as a collection of continuous band electrodes whose overpotentials are only a function of the x position along the channel: $\eta(x) = 2.08(x - x_0)$. The ECL intensity profile used for the calculations in Figure 2, which are discussed later, was extracted from Figure 1c along the line of pixels running through the tip of the triangular electrode. This ensures the highest ECL intensity resolution as a function of overpotential.

Relationship between an ECL Luminescence Micrograph and a Voltammogram. Bard and co-workers previously reported a direct correlation between faradaic current and ECL intensity as a function of potential.[13,14] In these studies, the potential of a microelectrode was slowly scanned in a solution containing $Ru(bpy)_3^{2+}$ and different co-reactants, including TPrA, and the current and ECL intensity were simultaneously recorded as a function of potential. Both the current and emission plots were

(18) Bard, A. J.; Faulkner, L. R. *Electrochemical Methods: Fundamentals and Applications*, 2nd ed.; John Wiley & Sons, Inc.: New York, 2001.
(19) Deiss, F. L.; LaFratta, C. N.; Symer, M.; Blicharz, T. M.; Sojic, N.; Walt, D. R. *J. Am. Chem. Soc.* **2009**, *131*, 6088–6089.

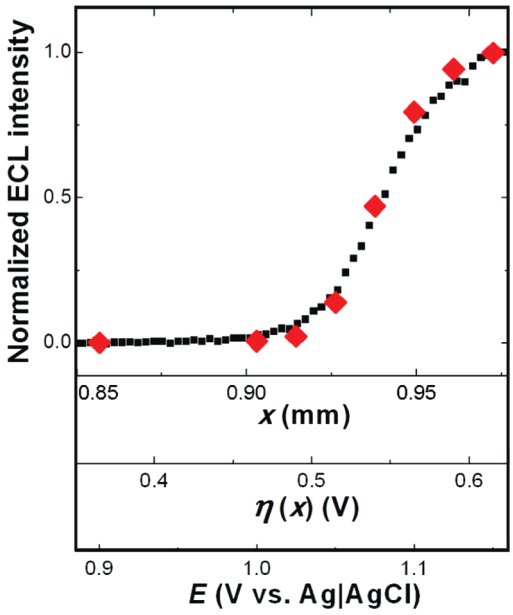

Figure 2. Black squares represent a cross-sectional ECL intensity profile along the direction of the applied electric field shown in Figure 1c. The horizontal axis was converted to overpotential ($\eta(x)$) using eq 4. The ECL profile was correlated to data obtained using a normal three-electrode cell, indicated by the red diamonds. See text for a complete explanation.

found to have sigmoidal shapes that could be fit by eqs 5 and 6, respectively.

$$i(E) = \frac{i_l}{1 + \exp\left[-\frac{nF}{RT}(E - E_{1/2})\right]} \quad (5)$$

$$I(E) = \frac{I_l}{1 + \exp\left[-\frac{nF}{RT}(E - E_{1/2})\right]} \quad (6)$$

Here, $i(E)$ and $I(E)$ are the current and the ECL intensity as a function of the potential E, i_l and I_l are the limiting current and the limiting ECL intensity, F is Faraday's constant, R is the gas constant, T is absolute temperature, n is the number of electrons transferred, and $E_{1/2}$ is the half-wave potential.

The potential gradient parallel to a BPE results in a continuum of potential differences between the electrode and the solution. This provides a means to transform the normal voltammetric experiment from the temporal domain to the spatial domain (along the plane of the BPE). Because the ECL emission intensity is directly related to the potential, it is possible to convert an ECL luminescence micrograph into a voltammogram.

The micrographs in Figure 3a show the luminescence intensity of ECL at the anode end of the triangular BPE for E_{tot} values of 23.0, 25.0, and 27.0 V, which are equivalent to V_0 values of 1.92, 2.08, and 2.25 V/mm, respectively. ECL profiles taken from these and other micrographs are plotted as a function of E_{tot} in Figure 3b. Both parts a and b of Figure 3 show that the illuminated electrode area increases as E_{tot} increases. As discussed earlier, this relationship is a consequence of the increasing overpotential gradient at the BPE/solution interface summarized by eqs 1 and 4. Because of the triangular shape of the BPE, the position of its equilibrium potential (x_0) does not

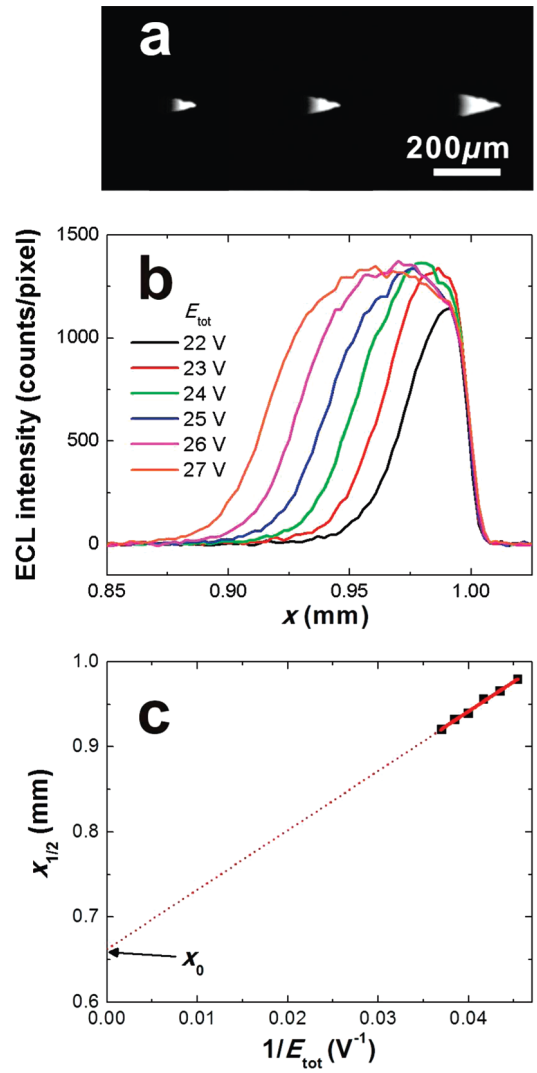

Figure 3. (a) ECL micrographs obtained at E_{tot} = 23.0, 25.0, and 27.0 V (left to right). (b) ECL intensity profiles obtained from luminescence micrographs like those shown in (a). To provide maximum spatial resolution, these profiles were obtained by plotting the line of pixels running through the BPE apex. The distance (x) is measured from the left edge of the BPE. (c) Plot of $x_{1/2}$, which is the location where the ECL intensity is one-half of its maximum value (extracted from part b) vs $1/E_{tot}$. The linear correspondence is expressed by eq 7.

shift significantly as a function of E_{tot}. This is important because it then becomes possible to extract the value of x_0 using the set of curves shown in Figure 3b. This is accomplished by rearranging eq 4, with $x = x_{1/2}$, where $x_{1/2}$ is the location on the electrode where the ECL intensity is one-half of the limiting ECL intensity (I_l). The result of this operation is eq 7.

$$x_{1/2} = \eta(x_{1/2})\frac{l_{channel}}{E_{tot}} + x_0 \quad (7)$$

Figure 3c is a plot of $x_{1/2}$ versus $1/E_{tot}$. It was obtained by combining eq 7 with the data in Figure 3b. The intercept of the best linear fit of the data points, which is the red line, yields x_0 = 0.66 mm. This means that the cathodic pole of the BPE extends from x_0 to the left end of the electrode and the anodic pole from x_0 to the right end.

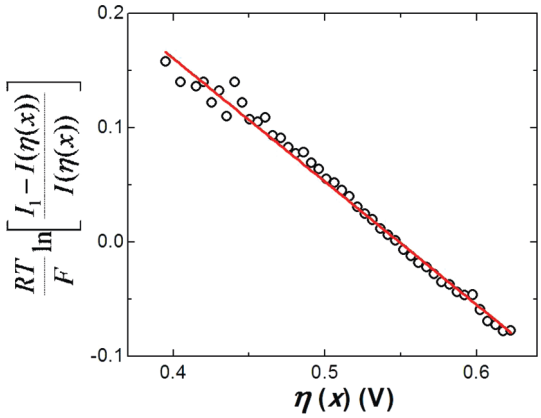

Figure 4. Plot of $(RT/F)\ln[(I_l - I(\eta(x)))/(I(\eta(x)))]$ vs $\eta(x)$. The data (open circles) were obtained from Figure 2 and fit (red line) using eq 8.

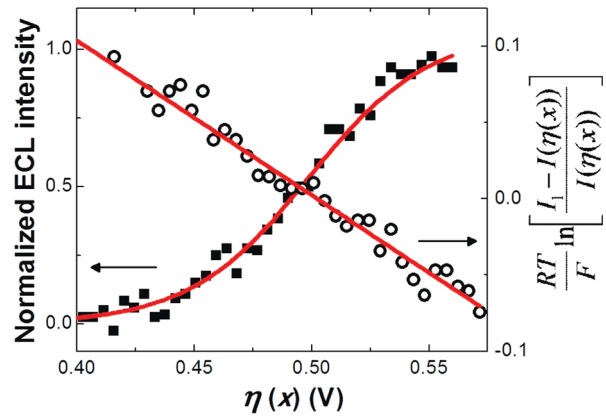

Figure 5. Filled squares represent an ECL intensity profile of $Ru(bpy)_3^{2+}$ with oxalate as its co-reactant. The open circles are a plot of $(RT/F)\ln[(I_l - I(\eta(x)))/(I(\eta(x)))]$ vs $\eta(x)$. The red lines were obtained by fitting the data to eqs 6 and 8. Conditions: $E_{tot} = 25.0$ V, and $V_0 = 2.08$ V/mm. The solution contained 5.0 mM $Ru(bpy)_3^{2+}$, 6.6 mM oxalate, and 0.10 M phosphate buffer (pH = 6.9).

In a previous study, which employed a rectangular electrode having a length equal to the longest lateral dimension of the triangular design used here, the value of x_0 was found to range from 0.78 to 0.82 mm depending on the value of E_{tot}.[6] The value of x_0 is lower for the triangular electrode because of the difference in surface areas of the cathodic and anodic ends of the electrode. This leads to a higher overpotential at the anodic end of a triangular electrode compared to an equivalent rectangular electrode. This in turn results in ECL being emitted over a greater length of a triangular electrode and hence to better resolution of the ECL intensity as a function of overpotential.

With the numerical value of x_0 in hand, eq 4 can be used to convert the horizontal axis of Figure 2 from x to $\eta(x)$. This conversion is important because it makes it possible to convert an ECL micrograph into a voltammogram. Next, we will show how various electrochemical parameters can be extracted from a snapshot voltammogram.

Extracting Electrochemical Parameters from a Snapshot Voltammogram. As discussed earlier, Bard and co-workers were able to fit plots of both current versus potential and ECL intensity versus potential using eqs 5 and 6. Because the ECL profile can be represented in terms of overpotential, $\eta(x)$ (Figure 2), it is possible to apply eq 6 to snapshot voltammetry by substituting $I(\eta(x))$ for $I(E)$, $\eta(x)$ for E, and $\eta_{1/2}$ for $E_{1/2}$ (eq 8).

$$\frac{RT}{F}\ln\left[\frac{I_l - I(\eta(x))}{I(\eta(x))}\right] = n(\eta_{1/2} - \eta(x)) \qquad (8)$$

Accordingly, the plot shown in Figure 4 can be generated using the values of $I(\eta(x))$ and I_l measured by snapshot voltammetry. The slope of the linear fit line of this plot represents the number of electrons transferred, n, and the intercept with the horizontal axis is $\eta_{1/2}$. Specifically, Figure 4 shows that $\eta_{1/2} = 0.549$ V versus $E(x_0)$ and that $n = 1.08$. The value of $n = 1$ represents the one-electron transfer corresponding to the oxidation of $Ru(bpy)_3^{2+}$ to $Ru(bpy)_3^{3+}$.[13]

To validate the method described in this paper, a snapshot voltammogram of another ECL system, consisting of $Ru(bpy)_3^{2+}$ and oxalate was obtained. As shown in Figure 5, the plot of the ECL intensity versus $\eta(x)$ has the same sigmoidal shape suggested by eq 6. Fitting the data to eq 8 results in $n = 1.01$ and $\eta_{1/2} = 0.502$ V versus $E(x_0)$ with $x_0 = 0.72$ mm for the oxalate system.

Comparison of Snapshot and Conventional Voltammograms. To directly compare snapshot and conventional voltammograms, a three-electrode microelectrochemical cell was used to record ECL emission intensity as a function of applied potential. The resulting data were then compared with results obtained by snapshot voltammetry. The experimental configuration used for this part of the study is provided in a previous report from our group.[6]

As described earlier, the triangular BPE is equivalent to a series of parallel microband electrodes, each of which experiences a different potential along its length. That is, the overpotential for the reaction of interest is a function of position along the x axis (Scheme 1) of the electrode. This information is equivalent to measuring ECL intensity at different applied potentials in a three-electrode cell. This point is underscored in Figure 2, where the red diamonds, representing data obtained from the three-electrode cell, are superimposed over the snapshot voltammogram obtained using the triangular BPE. This convergence makes it possible to convert $\eta(x)$ in Figure 2 to a conventional voltammogram having its potential axis expressed in terms of a conventional reference potential (E vs Ag/AgCl, Figure 2). This operation makes it possible to convert $\eta_{1/2}$ to a conventional half-wave potential: $E_{1/2} = 1.084$ V vs Ag/AgCl. This value is comparable to 1.0 V, which is estimated from plots of ECL intensity and current provided in the literature.[14] Thus, while snapshot voltammograms are most naturally referenced to overpotential, rather than to a normal reference electrode, once the equilibrium potential of the BPE is determined the potential axes can be interconverted.

SUMMARY AND CONCLUSIONS

The method of snapshot voltammetry relies on the difference in potential between a linear electric field in solution and a triangular-shaped electrode. The latter mimics the behavior of an array of band electrodes, but it has the advantage of maintaining a constant value of x_0 (the location where the electrode and solution potentials are the same), even when

the field gradient changes. Indeed, even though the potential of the BPE floats, it is possible to define the overpotential gradient by determining x_0. The overpotential gradient controls the driving force for electrochemical reactions taking place at different longitudinal locations along the triangular BPE. Importantly, we showed that it is possible to extract useful electrochemical parameters from a single snapshot voltammogram that are in good agreement with values measured by traditional voltammetry.

The significance of this work is that the geometric properties of a BPE provide the same information as that obtained using potential scanning methods. That is, the information present in a snapshot voltammogram resides in the spatial domain, whereas information obtained from conventional voltammetry resides in the time domain. Accordingly, the snapshot approach has the potential to be faster than normal voltammetry; for example, the snapshot data presented in this paper were obtained within 1.500 s. Another important outcome of the results presented here is that it should be straightforward to adapt the snapshot approach to a wireless electrode array format. Support for this claim comes from our previous finding that multiple wireless BPEs experiencing the same electric field can be controlled using just a single pair of driving electrodes.[1,4,5] Surface modification of the BPE in a large array with different probes, or fabrication of electrodes having different shapes, sizes, or metal substrates, could eventually lead to high-throughput voltammetric analyses because the data acquisition time is independent of the number of BPEs within the array.

ACKNOWLEDGMENT

We gratefully acknowledge financial support from the U.S. Army Research Office and the U.S. Defense Threat Reduction Agency (Grant No. W911NF-07-1-0330). We also thank the Robert A. Welch Foundation (Grant F-0032). B.Y.C. was partially supported by the Korea Research Fund Grant funded by the Korean Government (KRF-2008-357-C00091).

MAJOR SYMBOLS

$\eta(x)$	difference of potential between the electrode and the solution at position x, V
$\eta_{1/2}$	half-wave potential vs $E(x_0)$, V
$E(x)$	potential at position x inside the microfluidic channel, V
$E_{1/2}$	half-wave potential vs Ag/AgCl, V
E_{elec}	potential of a bipolar electrode, V
E_{eq}	equilibrium potential between the electrode and the solution, V
E_{tot}	applied potential difference between two driving electrodes, V
$i(E)$	current at potential E, A
i_l	limiting current, A
$I(\eta(x))$	ECL emission intensity at position x, counts
I_l	limiting ECL emission intensity, counts
$l_{channel}$	length of the microchannel, mm
V_0	electric field, V/mm
x	position on a bipolar electrode, mm
x_0	position on the bipolar electrode where the potential of the electrode and solution are equal, mm
$x_{1/2}$	position on the bipolar electrode where $I(\eta(x))$ is one-half of I_l, mm

SUPPORTING INFORMATION AVAILABLE

Detailed justification of the one-dimensional electric field model. This material is available free of charge via the Internet at http://pubs.acs.org.

Received for review March 31, 2010. Accepted May 13, 2010.

AC100846V